# Quartz SAR optically stimulated luminescence (OSL) dating of sands from Ulbjerg Klint, Central Jutland, Denmark

2020

Søren M. Kristiansen, Lars A. Larsen, Aayush Srivastava and Tim C. Kinnaird

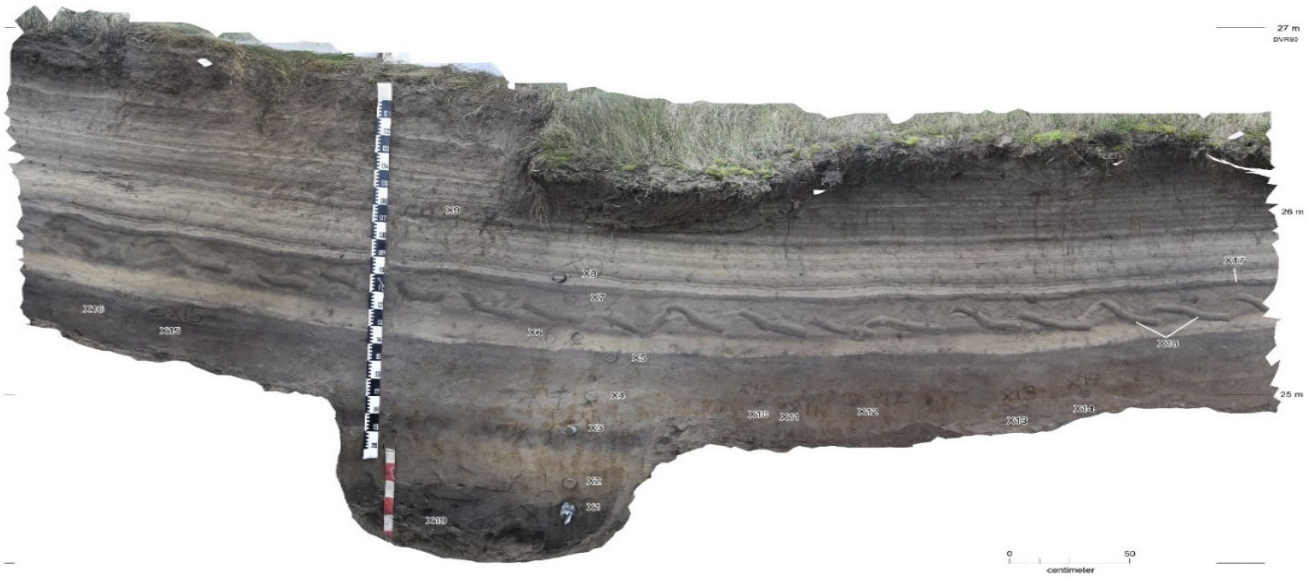


DEPARTMENT OF GEOSCIENCE
AARHUS UNIVERSITY

# Quartz SAR optically stimulated luminescence (OSL) dating of sands from Ulbjerg Klint, Central Jutland, Denmark

Søren M. Kristiansen, Lars A. Larsen, Aayush Srivastava and Tim C. Kinnaird[3,4]

[1]Department of Geoscience, Aarhus University, Denmark
[2]Viborg Museum, Denmark
[3]School of Earth & Environmental Sciences, University of St Andrews, Scotland
[4]School of Biological & Environmental Sciences, University of Stirling, Scotland

DEPARTMENT OF GEOSCIENCE
AARHUS UNIVERSITY

# Data


| | |
|---|---|
| Series title and number | Report from Department Geoscience |
| Title | Quartz SAR optically stimulated luminescence (OSL) dating of sands from Ulbjerg Klint, Central Jutland, Denmark |
| Subtitle | |
| Author(s) | Søren M. Kristiansen, Lars A. Larsen, Aayush Srivastava and Tim C. Kinnaird |
| Department | Geoscience |
| URL | http://www.geo.au.dk |
| Year of publication | October 2020 |
| Editing completed | October 2020 |
| Academic comment | Please note that the methodological descriptions may contain technical descriptions that are reused from previous reports and can be reused in future reports. We are grateful for help from Nina H. Nielsen, Pernille Trant, Ida-Emilie Nilsson and Thomas Ljungberg during the fieldwork, while background information was kindly provided by Mette Løvschal. The report for the archaeological fieldwork can be found at Viborg Museum, journal number: VSM 10569 Ulbjerg Klint. |
| Financial support | Viborg Museum covered Aarhus University' expenses for the fieldwork. Viborg Museum covered costs of the OSL analyses at University of St. Andrews, Scotland. It was funded by Agency for Culture and Palaces (Slots- og Kulturstyrelsen). |
| Please quote | Kristiansen, S.M., Larsen, L.A, Srivastava, A. & Kinnaird, T.C. Quartz SAR optically stimulated luminescence (OSL) dating of sands from Ulbjerg Klint, Central Jutland, Denmark. Report, Department of Geoscience, Aarhus University. 17 pages. |
| Version | 1 |
| Keywords | Aeolian sand, Archaeology, Climate, Plough marks, OSL dating, Drift sand, |
| Layout | Søren M. Kristiansen |
| Frontpage photo | The soil profile at Ulbjerg Klint. |
| Illustrations | Authors |

ISBN: 978-87-7507-488-4
DOI: 10.7146/aul.388

# Contents

# 1.0 Introduction

This report concerns optically stimulated luminescence (OSL) investigations of a soil profile at Ulbjerg Klint, Central Jutland, Denmark.

At this site, a minor landslide had exposed some unusually clear plough marks, which might contribute to the understanding of the first uses of the mould-board plough in southern Scandinavia (Larsen 2019).

The aims were first to date the plough marks, and secondly to date the first phase of the sedimentary archive of this site with a remarkable thick sequence of aeolian sand deposits with high archaeological and paleo-climate archive potential.

The report presents the OSL method, the results, a discussion and a conclusion, while the appendixes contains analytical description and a detailed soil profile and sampling description.

# 2.0 Sample details

The samples were taken in connection with an archaeological survey at the cliff Ulbjerg Klint approx. 20 km north of Viborg in Central Jutland, Denmark (Figure 1). The site is at the very top of a steep coastal cliff exposed towards the west in the Llmfjord area.

The archaeological survey was carried out in November 14, 2019 by Lars Agersnap Larsen, Viborg Museum in teamwork with Søren Munch Kristiansen, Department of Geoscience, Aarhus University. It was funded by Agency for Culture and Palaces (Slots- og Kulturstyrelsen). The report for the archaeological fieldwork can be found at Viborg Museum, journal number: VSM 10569 Ulbjerg Klint.

Samples X002, X006 and X008 from the soil profile shown in Figure 2 (profile description and close-up images see Appendix C and D) were submitted for OSL dating at the luminescence laboratories at the School of Earth and Environmental Sciences, University of St Andrews. These samples were assigned the laboratory codes CERSA464, 468 and 480 respectively. The samples were taken from an aeolian sandy layer (X002), on top of the lowermost A-horizon in a well-developed brownified soil in a parent material consisting of poorly sorted glacial sand, and from horizons of aeolian sand either side of the plough marks (X006 and X008, respectively).


Figure 1: Sampling site marked with red arrow. Coordinates are 519.263E/6.276.514N ETRS89/UTM zone 32N.


Figure 2: The soil profile at Ulbjerg Klint, Central Jutland, Denmark.

# 3.0 Equivalent dose determinations

All sample preparation and analyses were undertaken under safelight conditions at the luminescence laboratories at St Andrews.

Mineral preparation procedures similar to those used by Kinnaird et al. (2017) were used to extract HF-etched 'quartz' from the samples: samples were wet-sieved to obtain the 90 to 250 µm fraction; this fraction was then treated in 1M HCl for 10 mins, 40% HF for 40 mins, and a further 1M HCl for 10 mins; the 90 to 250 µm, HF-etched fractions were density separated in LST fastfloat solutions of 2.64 and 2.74 g $cm^{-3}$. The 90-250 µm, HF-etched, 2.64-2.74 g $cm^{-3}$ fractions were re-sieved at 150 µm, and the 150-250 µm fractions dispensed to 10 mm stainless steel discs for measurement.

Equivalent dose (De) determinations were made on sets of 24 aliquots using a single aliquot regenerative dose (SAR) OSL protocol (cf. Murray and Wintle, 2000; Kinnaird et al., 2017; appendix A). The OSL measurements were carried out using a Risø TL/OSL DA-20 automated dating system. Data reduction and De determinations were made in Luminescence Analyst v.4.31.9 and the package Luminescence in R. Luminescence behaviour was moderate: luminescence sensitivities were greater than 2600 counts $Gy^{-1}$, recycling ratios were within error of unity (1.02-1.04 ± 0.03-0.06) and dose recoveries were good (0.96-1.01 ± 0.03-0.07). Recuperation however, was relatively high, reflecting that the sediments are relatively young.

Individual De distributions were relatively homogenous, reflecting the aeolian mode of deposition. De distributions are shown as Kernel Density Estimate (KDE) and Abanico plots (Dietze et al., 2016) in Figure 3. For X002 and X008, the different statistical approaches for assimilating Des to obtain the apparent, or burial dose, yielded similar values: around 3.7 Gy for X002 and 0.5 Gy for X008. For X006, there is some divergence, hence the larger % uncertainty on the apparent dose estimate. For age assimilation (below), the weighted mean was used to assimilate Des to obtain the apparent dose.

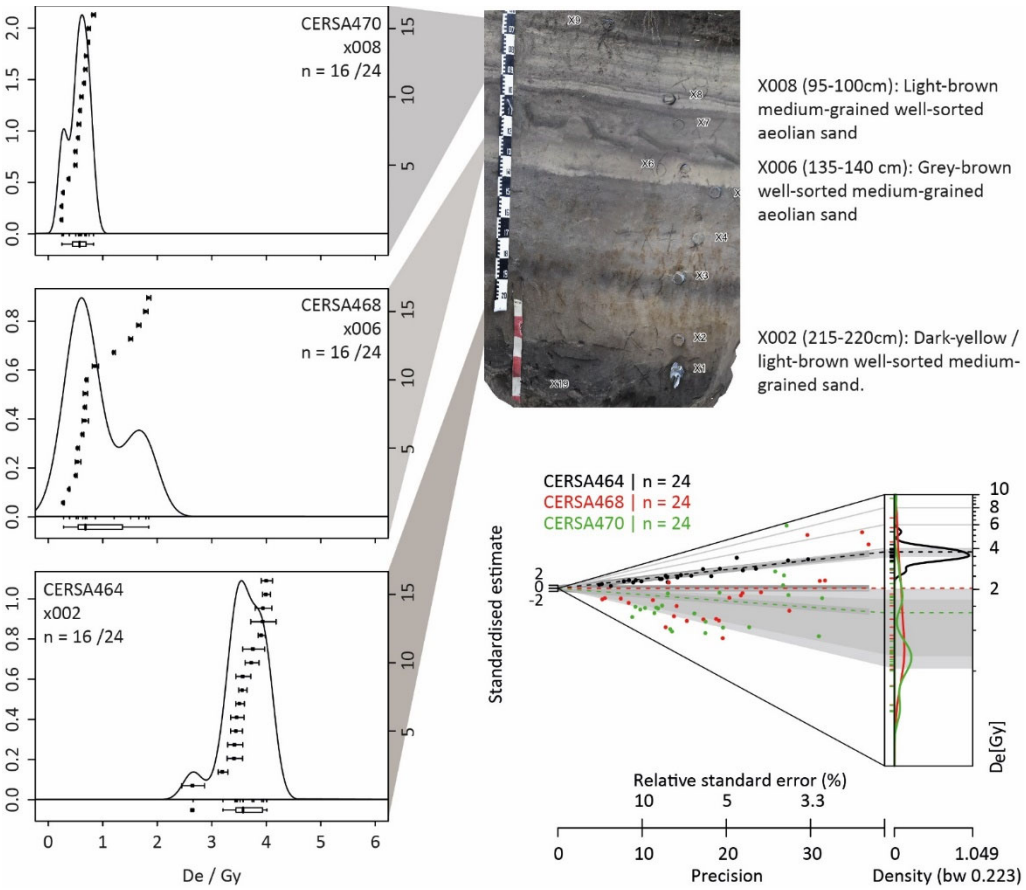


Figure 3: Equivalent dose distributions as Kernel Density Estimate plots for samples X002, X006 and X008, shown relative to the stratigraphy of the Ulbjerg Klint section.

# 4.0 Dose rate determination

Dose rates to the HF-etched quartz fraction were assessed by high-resolution gamma spectrometry (HRGS). HRGS measurements were performed at the Environmental Radioactivity Laboratory (ERL; UKAS Testing Lab 2751) in the School of Biological and Environmental Sciences at the University of Stirling.

All sampling handling, processing and analyses were undertaken in accordance, and in compliance with ERL protocols LS03.1, 03.2 & 03.6 and LS08. The samples were sealed for four weeks prior to final counting.

The HRGS measurements were performed on a High Purity Germanium detector. Standard laboratory efficiency calibrations were used, derived from GE Heathcare Ltd QCY48 Mixed Radionuclide Spike and DKD RBZ-B44 $^{210}$Pb spike. All absolute efficiency calibrations were corrected for variations in sample density and matrix. The decay reference date was the 3rd of December 2019. Nuclide specific estimates for K, and the U and Th series were used to estimate mean activity concentrations (Bq kg$^{-1}$) and elemental concentrations (% K and ppm U and Th) for the parent activity (Table 1). These data were used to determine infinite matrix doses for , and radiation (Table 1), using the conversion factors of Guérin et al. (2011), grain-size attenuation factors of Mejdahl (1979) and attenuated for water using the moisture content values listed in Table 1. External $\dot{D}_{\alpha}$ dose rates were ignored as the irradiated portion of quartz was removed by HF-etching. The contribution from the cosmic dose was calculated following Prescott and Hutton (1994), as a function of geographic location (altitude, longitude and latitude) and burial depth.

*Table 1: Radionuclide concentrations, infinite matrix dose rates (top) and total effective dose rate (bottom) for CERSA464, 468-470.*

| Field ID | CERSA ID | Radionuclide concentrations | | | Dry infinite matrix dose rates / mGy a$^{-1}$ | | |
|---|---|---|---|---|---|---|---|
| | | K / % | U / ppm | Th / ppm | Alpha, α | Beta, β | Gamma, γ |
| X002 | 464 | 1.31 ± 0.15 | 0.55 ± 0.09 | 1.02 ± 0.1 | 2.29 ± 0.25 | 1.06 ± 0.12 | 0.44 ± 0.04 |
| X006 | 468 | 1.41 ± 0.13 | 0.85 ± 0.06 | 1.37 ± 0.12 | 3.38 ± 0.19 | 1.18 ± 0.11 | 0.51 ± 0.03 |
| X007 | 469 | 1.42 ± 0.13 | 0.84 ± 0.07 | 1.37 ± 0.1 | 3.36 ± 0.20 | 1.19 ± 0.11 | 0.51 ± 0.03 |
| X008 | 470 | 1.38 ± 0.16 | 1.31 ± 0.13 | 1.59 ± 0.14 | 4.83 ± 0.38 | 1.22 ± 0.13 | 0.57 ± 0.04 |

| Field ID | CERSA ID | Water content / % | Effective beta dose rate / mGy $a^{-1}$ | Effective gamma dose rate / mGy $a^{-1}$ | Contribution from cosmic dose / mGy $a^{-1}$ | Total effective dose rate / mGy $a^{-1}$ |
|---|---|---|---|---|---|---|
| X002 | 464 | 13 ± 4 | 0.92 ± 0.11 | 0.38 ± 0.10 | 0.14 ± 0.01 | 1.50 ± 0.15 |
| X006 | 468 | 16 ± 5 | 1.00 ± 0.1 | 0.43 ± 0.08 | 0.15 ± 0.02 | 1.65 ± 0.13 |
| X007 | 469 | 15 ± 5 | 1.02 ± 0.1 | 0.44 ± 0.07 | 0.16 ± 0.02 | 1.68 ± 0.13 |
| X008 | 470 | 17 ± 4 | 1.02 ± 0.12 | 0.46 ± 0.08 | 0.16 ± 0.02 | 1.71 ± 0.14 |

# 5.0 Age determination

A luminescence age is the quotient of the stored dose (in Gy) over the effective environmental dose rate (in mGy $a^{-1}$).

Three samples were age determined: X002, X006 and X008.

Stored dose estimates in the range 3.7 to 0.5 Gy, combined with the dose rate estimates to the Ulbjerg Klint quartz at 1.5 to 1.7 mGy $a^{-1}$, correspond to depositional ages between 2.44 ± 0.25 ka and 0.27 ± 0.04 ka (420 ± 250 BC and AD 1750 ± 40; Table 3).

The sandy layer above the lowermost A horizon at the base of the Ulbjerg Klint section have been dated to 2.44 ± 0.25 ka (420 ± 250 BC). This provides TAQ for the formation of the lowermost soil.

The aeolian sands either side of the plough marks are dated to 0.36 ± 0.10 ka (AD 1660 ± 100) and 0.27 ± 0.04 ka (AD 1750 ± 40). This provide TPQ and TAQ for the horizon containing the plough marks.

*Table 2: Age determinations.*

| Field ID | CERSA ID | Total effective dose rate / mGy $a^{-1}$ | Stored dose / Gy | Age / ka | Calendar years |
|---|---|---|---|---|---|
| X002 | 464 | 1.50 ± 0.15 | 3.66 ± 0.09 | 2.44 ± 0.25 | 420 ± 250 BC |
| X006 | 468 | 1.65 ± 0.13 | 0.60 ± 0.15 | 0.36 ± 0.10 | AD 1660 ± 100 |
| X008 | 470 | 1.71 ± 0.14 | 0.46 ± 0.06 | 0.27 ± 0.04 | AD 1750 ± 40 |

# 6.0 Discussion

As recorded by the multiple aeolian sandy layers in the profile (Figure 2), this site at an exposed coastal cliff towards the Limfjord (Lovns Bredning) has experienced several periods where the protecting vegetation have been removed from the surface and drift sand and problems for the farming occurred. Three of these episodes are dated.

The wind-deposited sandy layer below the plough mark layer is from the 17th century, while the wind-deposited sandy layers sealing the attempt to plough this site is from the 18th century. This suggest that the drift sand covered the westernmost parts of an east-west orientated field system. This field system with ridge and furrows is today not visible in the field but in digital elevation models (Figure 4). The drift sand were deposited within short time (year-decade) because only very thin humus layer was developed, and no bioturbation of the stratified sediment was detected in the sandy layers. These dates are comparable to the recent results from Breuning-Madsen et al (2018) from southern Denmark. Here in a single event, about 400 years ago, a many square km large deflation area sank about 2 to 3 m and huge quantities of drift sand was deposited towards the east. Aeolian sand activities along the North Sea cost seems more distributed in time and are maybe more related to the Atlantic ocean' oscillations (e.g., Szokornik et al., 2008, Goslin et al., 2019). The findings from Ulbjerg supplements the finding by Breuning-Madsen et al. (2018) and stress that significant in-land drift sand problems took place in the early 17th century in Denmark. Furthermore, it suggest that research not only in the Little Ice Age but also in archaeology have to focus on the coldest years and decades during the Holocene, as the recent revised ice-core chronologies (Sigl et al., 2015) show that 8 of the 40 coldest years and 2 of the 12 coldest decades actually took place in the early 17th century. All of these events were consequences of volcanic eruptions in a period of declining temperatures globally (Neukom et al., 2019).

The sample from the first aeolian sand above lower-most soil developed in glacial sediments revealed that, within the uncertainty of the OSL dating methods, the wind-deposited sand sealing this surface was dated to the 5th century BCE, i.e. at or slightly after the transition (500 BCE) between the Danish late Bronze Age to the pre-Roman Iron Age. Here, a period of deforestation (around 500 BC) at the lakes Solsø and Skånsø is evident in the local pollen diagrams but it was too short to trigger a migration of beech trees into the western Jutland area (Odgaard, 1994). Interestingly, though, recent research have shown that the largest volcanic eruption in the last 2500 years was in year 425 BCE with one top 12 cold decade as a conse-

quence (Sigl et al., 2018). More research with a high-definition dating approach have thus to focus on this period of transition as evidenced in the climatic and archaeological records.

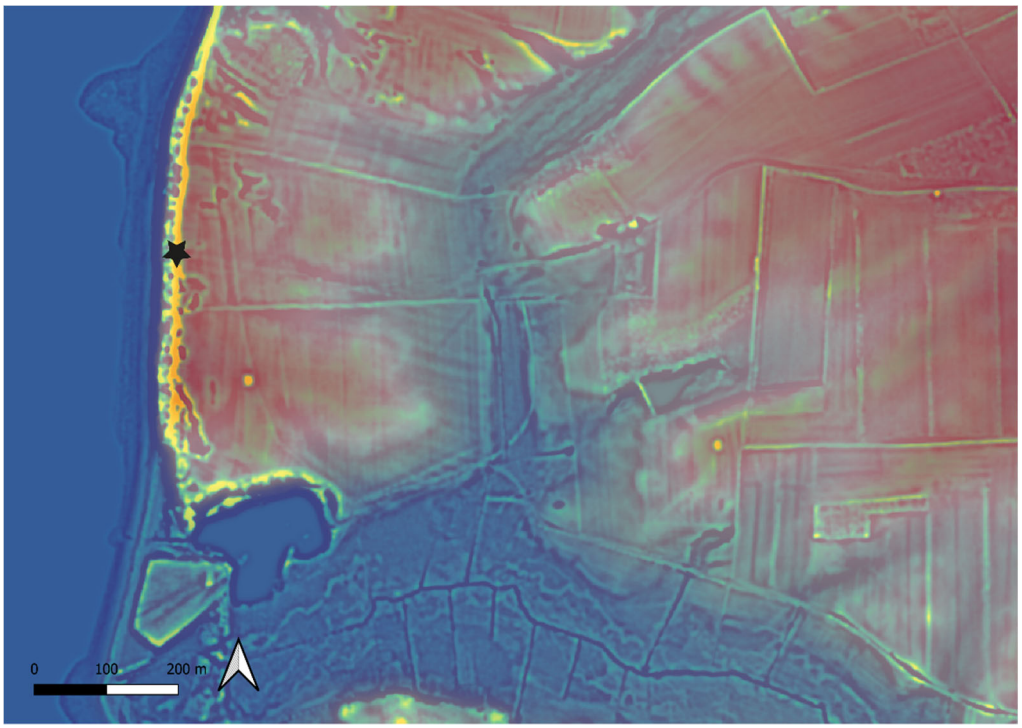


*Figure 4. The ridge and furrow field system found south, east and north of the sampling site at Ulbjerg Klint is seen as east-west orientated lines (darker are furrows, paler are ridges) in the landscape today. The images is a combined residual relief model (yellow colours) to enhance the 10-30 cm difference in height between the ridges and the furrows, on top of a digital elevation model coloured by blue (0 m a.s.l.) to red (35 m). Residual relief model adapted from Stott et al. (2018). Sampling site marked with black star.*

# 7.0 Conclusions

Combined, the determined OSL ages reveal that over a 2500 years period the vegetation on this exposed coastal cliff was removed several times with episodes of drifting sand as a consequence. The first aeolian sand layer is dated at or slightly after 5th century BCE, i.e. around the transition between the Danish late Bronze Age to the pre-Roman Iron Age. The aeolian sand layer with the clear plough marks is from the 17th century CE, i.e. in the Little Ice Age. Due to the limited number of OSL dated samples, no additional climatic or land use indications could be established.

# 8.0 References

Breuning-Madsen, H.; Bird, K. L.; Balstrøm, T.; Elberling, B.; Kroon, A.; Lei, E. B., 2018, Development of plateau dunes controlled by iron pan formation and changes in land use and climate. *Catena* 171, 580-587.

Dietze, M., Kreutzer, S., Burow, C., Fuchs, M. C., Fischer, M. and Schmidt, C., 2016, The Abanico plot: visualising chronometric data with individual standard errors. *Quaternary Geochronology*, 31, p. 12-18.

Goslin, J.; Gałka, M.; Sander, L.; Fruergaard, M.; Mokenbusch, J.; Thibault, N.; Clemmensen, L. B., Decadal variability of north-eastern Atlantic storminess at the mid-Holocene: New inferences from a record of wind-blown sand, western Denmark. Global and Planetary Change 2019, 180, 16-32.

Guérin, G., Mercier, N. and Adamiec, G., 2011, Dose-rate conversion factors: update. *Ancient TL*, 29, p. 5-8.

Kinnaird, T. C., Dawson, T., Sanderson, D. C. W., Hamilton, D., Cresswell, A. and Rennel, R., 2017, Chronostratigraphy of an eroding complex Atlantic round house, Baile Sear, Scotland. *Journal of Coastal and Island Archaeology*, 14 (1), p. 46-60.

Kreutzer, S., Dietze, M., Burow, C., Fuchs, M.C., Schmidt, C., Fischer, M. and Friedrich, J., 2017. Luminescence: Comprehensive luminescence dating data analysis. R package version 0.7. 3.

Larsen, L.A., 2019, The early introduction of the moldboard plow in Denmark. Agrarian technology and the medieval elite. *Nordic Elites in Transformation c. 1050-1250*, Vol. 1: Material resources (eds. Bjørn Poulsen, Helle Vogt & Jón Viðar Sigurðsson), p. 80-106.

Mejdahl, V., 1979, Thermoluminescence dating: Beta-dose attenuation in quartz grains. *Archeometry*, 29(1), p. 61-72.

Murray, A. S. and Wintle, A. G., 2000, Luminescence dating of quartz using an improved single-aliquot regenerative-dose protocol. *Radiation Measurements,* 32(1), p. 57-73.

Neukom, R.; Barboza, L. A.; Erb, M. P.; Shi, F.; Emile-Geay, J.; Evans, M. N.; Franke, J.; Kaufman, D. S.; Lücke, L.; Rehfeld, K.; Schurer, A.; Zhu, F.; Brönnimann, S.; Hakim, G. J.; Henley, B. J.; Ljungqvist, F. C.; McKay, N.; Valler, V.; von Gunten, L.; Consortium, P. k., Consistent multidecadal variability in global temperature reconstructions and simulations over the Common Era. Nature Geoscience 2019, 12 (8), 643-649.

Odgaard, B. V., The Holocene vegetation history of northern West Jutland, Denmark. *Opera Botanica* 1994, 123, 1-171.

Prescott, J. R. and Hutton, J. T., 1994, Cosmic ray contributions to dose rates for luminescence and ESR dating: Large depths and long-term time variations. *Radiation Measurements*, 23(2), p. 497-500.

Stott, D.; Kristiansen, S. M.; Sindbæk, S. M., Searching for Viking Age Fortresses with Automatic Landscape Classification and Feature Detection. Remote Sensing, 2019, 11 (16).

Szkornik, K.; Gehrels, W. R.; Murray, A. S., Aeolian sand movement and relative sea-level rise in Ho Bugt, western Denmark, during the `Little Ice Age'. The Holocene 2008, 18 (6), 951-965.

# 9.0 Appendixes

## Appendix A: Equivalent dose determinations

All OSL measurements were carried out using a Risø TL/OSL DA-20 automated dating system, equipped with a $^{90}Sr/^{90}Y$ -source for irradiation (dose rate at time of measurement, 0.10 Gy/s) blue LEDs emitting around 470 nm and infrared diodes emitting around 830 nm for optical stimulation. OSL was detected through 7.5 mm of Huoya U-340 filter and detected with a 9635QA photomultiplier tube. OSL was measured at 125°C for 60 s. The OSL signals, *Ln* and *Lx*, used for equivalent dose (*De*) determinations were obtained by integrating the OSL counts in the first 2.4 s and subtracting an equivalent signal taken from the last 9.6 s.

De determinations were determined using a single-aliquot regenerative dose (SAR) method (Kinnaird et al., 2017; Murray and Wintle, 2000), which allows for an independent estimate of De to be generated for each aliquot measured. The SAR technique involves making a series of paired measurements of OSL intensity - the *Ln* and *Lx* outlined above, and the response to a fixed test dose, *Tn* and *Tx*. Each measurement is standardised to the test dose response determined immediately after its readout, to compensate for observed changes in sensitivity during the laboratory measurement sequence. De values are then estimated using the corrected OSL intensities *Ln/Tn* and *Lx/Tx* and the interpolated dose-response curve.

This was implemented here, using four regenerative doses (nominal doses of 2.9, 5.8, 11.7 and 35.1 Gy), with additional cycles for zero dose, repeat or 'recycling' dose (2.9 Gy) and IRSL dose (2.9 Gy). The zero dose point is used to monitor 'recuperation', thermally induced charge transfer during the irradiation and preheating cycle. The repeat dose - a repeat of the initial regeneration dose - is used to calculate the 'recycling ratio', a test of the internal consistency of the growth curve. The IRSL response check is included to assess the magnitude of non-quartz signals. To ensure that there was no dependency of De or sensitivity on preheat conditions, five preheat temperatures were explored from 220 to 260°C in 10°C increments.

Data reduction and De determinations were made in Luminescence Analyst v.4.31.9. Individual decay curves were scrutinised for shape and consistency. Dose response curves were fitted with an exponential function, with the growth curve fitted through zero and the repeat recycling points. Error analysis was determined by Monte Carlo Stimulation.

Representative OSL decay curves for both the natural and regenerated signals, together with the corresponding dose response curve are shown in figure S2-1 to S2-4.

Fig A-1: Representative decay and dose response curves from CERSA464 (X002) #1

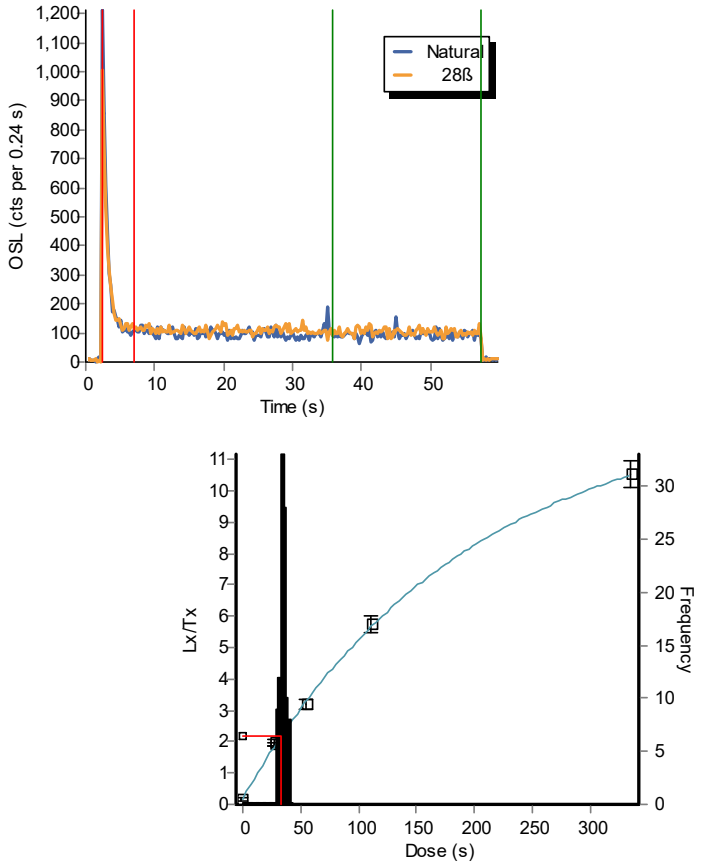

Fig A-2: Representative decay and dose response curves from CERSA468 (X006) #16

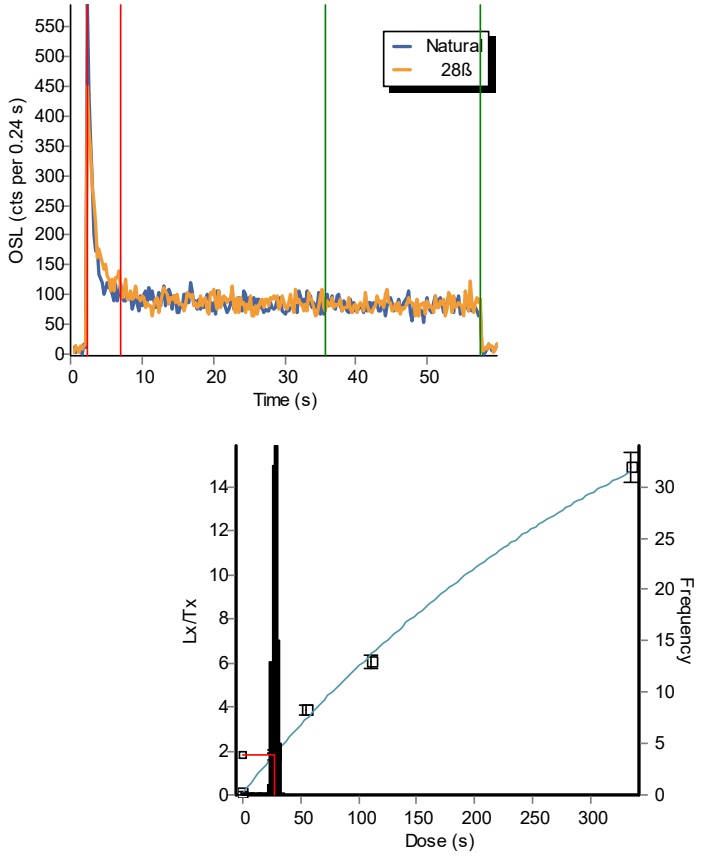

Fig A-3: Representative decay and dose response curves from CERSA470 (X008) #16

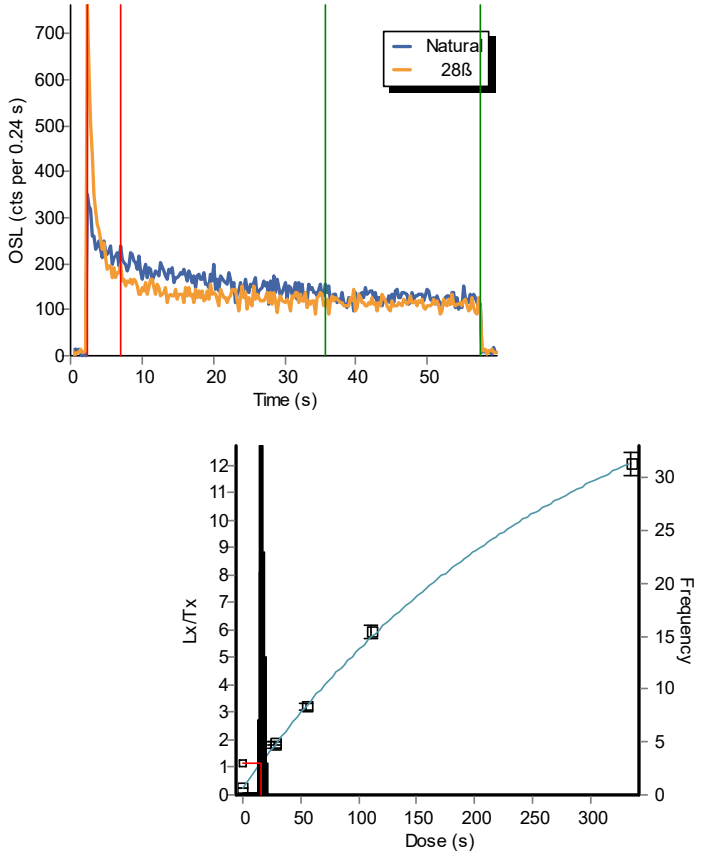

# Appendix B: Equivalent dose distributions

OSL SAR dating utilises extracted quartz from the samples to determine the radiation dose experienced by the sediments since their last zeroing event assumed to be by exposure to light prior to final deposition, the burial dose, *Db*. To obtain a depositional age, it is necessary to reduce each samples *De* distribution to a single *Db*.

### S3.1. Internal consistency of quartz OSL SAR data

Aliquots were rejected from further analysis if they failed sensitivity checks (based on test dose response), SAR acceptance criteria checks, or had significant IRSL response coupled with anomalous luminescence behaviour. Luminescence sensitivities (luminescence per unit dose, counts $Gy^{-1}$), recycling ratios, recuperation values, IR response (%) and dose recovery ratios are listed in table S3.1.

### S3.2. Distribution analysis

The distributions in equivalent dose values, for those aliquots which satisfied the SAR selection criteria, were examined using Kernel Density Estimate (KDE) plots and Abanico plotting methods (Dietze et al., 2013). KDE and Abanico Plots are for samples CERSA464, 468 and 470 are provided in figure 2.

*Table S3.1: SAR quality criteria, 150-250µm quartz*

| Field ID | CERSA no. | Sensitivity/ counts $Gy^{-1}$ | Recuperation /% | Recycling ratio | IRSL response / % | Dose recovery ratio |
|---|---|---|---|---|---|---|
| X002 | 464 | 2580 ± 1830 | 8 ± 8.1 | 1.03 ± 0.06 | 5.3 ± 15.8 | 1.01 ± 0.07 |
| X006 | 468 | 8430 ± 4900 | 35 ± 9.4 | 1.02 ± 0.03 | 52.0 ± 27.7 | 0.97 ± 0.03 |
| X008 | 470 | 15900 ± 18660 | 41.3 ± 10.2 | 1.04 ± 0.04 | 49.4 ± 25.2 | 0.96 ± 0.04 |

# Appendix C: Soil profile description at Ulbjerg Klint

| Layer | Horizon | Description |
|---|---|---|
| 1 | C1 | 0-92 cm depth. Horizontal layers of sand of 1-10 cm thickness of shifting light yellow (C-horizon drift sand) and grey-yellow (org. rich A-horizon drift sand). Medium, well-sorted aeolian sand. Many thin roots (<1 mm). Some bioturbation. The upper ca. 10 cm has some recent seashells and some barbwire incorporated. A week soil development (bleached sand grains) has begun in the top 10 cm. Abrupt boundary to layer 2. |
| 2 | Apb2 | 92-120 cm. Medium well-sorted aeolian sand. Light brownish. Some fine roots. Few roots up to 5 mm. The layer with clear mouldboard plough marks have some of the layers turned up side down. Only one ploughing seen, with an east-west orientation. Abrupt internal layer boundaries. Interpretation: shortly after a drifting sand episode, it was plough but a new drift sand episode took place now with greyish (mould/A-horizon) drift sand covering everything. Abrupt boundary to layer 3. |
| 3 | C2 | 120-133 cm. Yellow medium, well-sorted sand, aeolian sand. Few roots of which some are 2-3 mm. Some bioturbation but clear layering. A few org. rich Ø1-1½ cm channels from layer 4a which are interpreted as earthworm channels. Boundary to layer 4 is abrupt and wavy. |
| 4a | Apb3 | 133-140 cm. Greyish well-sorted medium aeolian sand. Very homogenous A-horizon. No redox features. The difference from layer 4b is a ca. 2 cm thick diffuse non-continuous layer of sand. Few macroscopic visible pieces of charcoal. A weakly wavy boundary to layer 4b. |
| 4b | BC3 | 140-180 cm. Grey-brown and few paler mottles in well-sorted medium aeolian sand. Psudogley in ca. 10% of the horizon – especially in the central part – with diffuse red-black Fe-Mn non-cemented masses. This pseudogley including the more greyish colours is maybe developed in a more yellow drift sand? Few charcoal fragments in a 5-10 cm bred zone suggest a more stable surface at ca. 160-170 cm. Layer 4b had somewhat more org. C in the upper 5-10 cm relative to layer 4a. Boundary to layer 5 abrupt. |
| 5 | Ab4 | 180-188 cm. Dark brownish grey well-sorted medium aeolian sand. Has a high organic C content and stains the fingers (rich in fine charcoal?). Relatively homogenous with ca. 15% pseudo-gley similar to the description of layer 4b. Boundary to layer 6 is sharp to diffuse in some places. |
| 6 | C4 | 188-223 cm. Dark yellowish to light brownish well-sorted medium (drift) sand. Some pseudogley. Homogenous layer. Few larger stones (Ø<10 cm). Abrupt boundary to layer 7. |
| 7 | Ap5 | 223-245 cm. Brownish to black. A well-developed mould layer (A-horizon) with many up to 5-8 cm stones. well-sorted medium sand in the uppermost c. 6-10 cm. Interpreted as drift sand with a significant higher organic C content relative to layer 6. Relativt homogen. The upper part is the Late-/periglacial soil surface. Unclear if there is ploughing in it but a p is added to the horizon designation (Apb) as the laye ris unusual thick compared to any other reported Bronze Age surface soils on sandy parent material in this part of Denmark. Diffuse boundary to layer 8. |
| 8 | C5 | 245-minimum 350 cm. Yellow-grey meltwater sand. Poorly sorted. Very stone rich in the top 20-30 cm only, but gravel in thin layers. |

***Foot notes:***

- *Sampling date: 2.12.2019.*
- *Description: Pernille Trant, Ida-Emilie Nilson, Søren M. Kristiansen*

- *The light was very poor this over-casted winter day. Hence no soil colours in the field.*
- *It is likely that more soil surface than the ones described present in the ca. 223 cm thick drift sand deposit, but these were not well-expressed in the profile and represents hence shorter stability periods than the layers described above.*
- *No artefacts found and only some charcoal in layer 4b (could not be determined as to species in the lab) so not radiocarbon dated.*
- *The lowermost soil development in the fluvio-glacial deposit is interpreted as naturally only, although the A horizon (Ap5) is very thick compared to anything else seen in this part of western Denmark.*

## Appendix D: additional profile images

*Figure A1. Overview of the sampled and described profile for OSL dating.*

*Figure A2. Close-up of the samples for OSL dating.*


*Figure A3. Close-up of the samples for OSL dating.*